NOAA Technical Memorandum ERL FSL-21

IMPACT OF MULTICHANNEL PASSIVE MICROWAVE RADIOMETER DATA ON THE LAPS MOISTURE ANALYSIS

Daniel Birkenheuer

Forecast Systems Laboratory
Boulder, Colorado

January 1998

UNITED STATES DEPARTMENT OF COMMERCE

William M. Daley
Secretary

NATIONAL OCEANIC AND ATMOSPHERIC ADMINISTRATION

D. JAMES BAKER
Under Secretary for Oceans and Atmosphere/Administrator

Environmental Research Laboratories

James L. Rasmussen
Director

NOTICE

Mention of a commercial company or product does not constitute an endorsement by NOAA Environmental Research Laboratories. Use for publicity or advertising purposes of information from this publication concerning proprietary products or the tests of such products is not authorized.

For sale by the National Technical Information Service, 5285 Port Royal Road, Springfield, Virginia 20061

CONTENTS

List of Figures

IMPACT OF MULTICHANNEL PASSIVE MICROWAVE RADIOMETER DATA ON THE LAPS MOISTURE ANALYSIS

Daniel Birkenheuer

ABSTRACT. The Local Analysis and Prediction System (LAPS) contains a specific humidity analysis component. One data source used in the analysis is real-time total column moisture measured by a multichannel passive radiometer, which provides total precipitable water data every two minutes from two sites in the analysis domain. This paper compares two datasets acquired over the past year and shows that radiometer data have a measurable positive impact on the LAPS moisture analysis.

1. INTRODUCTION

The LAPS moisture analysis temporarily lost its radiometer input in November 1994 due to a reconfiguration of the data sources within the Forecast Systems Laboratory (FSL). Radiometer data represent a real-time measurement of total column moisture measured by a multichannel passive radiometer at two sites in the analysis domain (Westwater 1993). During this hiatus, comparisons of LAPS moisture output from the quasi-operational, real-time run with and without this data source was made using archived statistics from before and after data loss. Granted these datasets are not free from other possible differences, as in weather type, or possible algorithm improvements. In this sense, this is not meant to be the *final* word on radiometer impact, however, it is worth looking at these data to get a good estimate how total moisture affects the LAPS specific humidity analysis from a statistically significant number of cases. These results are relevant in light of the new Global Positioning System (GPS) data that will be available in the future. Similar analysis impact to LAPS would be expected from a data source such as GPS.

2. LAPS

The specific humidity module is one of 17 major LAPS algorithms that span everything from data preparation and quality control to actual analysis. Within this dataset, there are four major processes responsible for merging data and negotiating the final output field of atmospheric state variables we consider analysis. In addition to state variables, LAPS also addresses highly specific analyses of special interest, such as aircraft icing threat. McGinley et al. 1991 details the LAPS analysis, and here we review the LAPS specific humidity algorithm, paying special attention to the radiometer step.

3. DATA SOURCES

The major inputs to the LAPS specific humidity (SH) analysis are model moisture analyses (or forecasts); LAPS surface pressure, temperature, and dewpoint temperature fields; radiometer column water vapor data; LAPS three-dimensional cloud and temperature analyses; and GOES sounding infrared (IR) radiance fields.

3.1 Model Moisture

The basis for the LAPS moisture background field is FSL's Mesoscale Analysis and Prediction System (MAPS). Other forecast output that have been used include the Rapid Update Cycle (RUC) and the Nested Grid Model (NGM) moisture analysis/forecast fields. Any three-dimensional model field can be used as long as it is interpolated to the LAPS pressure coordinates and 10 km grid. The interpolation is done in steps. First, a temporal interpolation is calculated. The best combination of background model analysis and forecast fields are interpolated in time to synthesize a field for the LAPS analysis hour of interest in the model horizontal and vertical coordinate system. Then, an interpolation from model vertical coordinates to the LAPS pressure coordinate is performed. Following this a horizontal interpolation occurs from which the LAPS 10 km grid is filled from the coarser model background grid.

3.2 LAPS Three-Dimensional Cloud and Temperature

The LAPS cloud analysis operates hourly and uses a height vertical coordinate with 42 levels. The analysis produces cloud fraction ranging from zero to one, where one represents 100% cloudiness. Data sources for the analysis are conventional surface observations of cloud base and cover, window channel data (11.2 μm infrared data from GOES), Aeronautical Radio Incorporated (ARINC) Communications Addressing and Reporting System (ACARS) aircraft reports of clouds and icing, and radar data. An expanded description of the cloud analysis may be found in McGinley and Albers (1991).

3.3 LAPS Surface T, p, and T_d

The LAPS surface analysis provides three input fields: surface temperature, pressure, and dewpoint temperature. The analysis combines a Barnes analysis with a Laplacian minimization to smooth the resultant fields. The methods summarized here are detailed in McGinley et al. (1991). The T_d field defines the boundary layer moisture. The surface temperature and pressure are used in the computation of boundary layer depth, as will be explained later.

3.4 Radiometer data

Real-time total column water vapor measurements are available at two locations in the LAPS domain from ground-based passive microwave radiometers operated by NOAA's Environmental Technology Laboratory (Westwater 1993). These data scale the water vapor fields by fitting analyzed integrated water to this real-time data source. Radiometer data have been shown to be of high quality with RMS errors of 0.03 cm when compared to Cross-chain Loran Atmosphere Sounding Systems (CLASS) sounding data and even lower values when compared with Raman lidar data (Han et al. 1994).

3.5 GOES Moisture Fields

By far, the data providing the most spatial detail are water vapor fields derived from satellite measurements. This aspect of the analysis was run on the earlier versions of LAPS using data from the GOES-7 dwell sounding scans. Their frequency ranged from 90 minutes to once every 2 or 3 days depending on the rapid interval scanning constraints that preclude dwell sounding ingest. GOES provided data each hour in 12 infrared spectral channels (or bands) covering the continental United States. This procedure operated quasi-operationally at FSL and is currently planned to be adapted to run hourly using GOES-8 data once they are available.

The exact technique is documented in Birkenheuer 1991. In short, LAPS derives three separate layers of precipitable water (LPW) moisture fields from sounder quality GOES IR radiance fields in cloud-free regions. The partition levels for the layers are 780 and 640 defining three layers: surface to 780 hPa, 780 to 640 hPa, and above 640 hPa.

4. ALGORITHM

The LAPS specific humidity algorithm can be divided into fundamental parts: boundary layer treatment, radiometer (GPS) water vapor adjustment, cloud saturation, horizontal shape matching, cloud saturation, and quality control.

4.1 Boundary Layer Moisture

The LAPS surface and three-dimensional temperature analyses together diagnose boundary layer moisture. A method modeled after Rogers and Schwartz (1991) examines the value of the Brunt-Vaisala frequency computed from ground level upward. The Brunt-Vaisala frequency N^2 is computed from

$$N^2 = \left(\frac{g}{T}\right)^2 \frac{p}{R}\left(\frac{kT}{p} - \frac{\partial T}{\partial p}\right), \tag{1}$$

where g is gravitational acceleration, T is the temperature, p the pressure, R the gas constant of air, and $k = R/c_p$ with c_p the specific heat of air at constant pressure. The level at which N^2 changes sign indicates a change from an unstable regime to one of static stability. The interpolated level of zero Brunt-Vaisala frequency defines the top of the mixed (boundary) layer. Next the surface moisture as diagnosed by the LAPS surface dewpoint (T_d) analysis is mixed upward to the top of this diagnosed level.

4.2 Total Column Water Vapor

Real-time total column water vapor is used to scale the water vapor above the boundary layer. The integrated specific humidity (SH g kg^{-1}) is related to total column precipitable water (TPW g cm^{-2}) as:

$$TPW = \int_{b}^{s} \frac{SH}{100g} dp + \zeta \int_{100}^{b} \frac{SH}{100g} dp \qquad (2)$$

where g is the gravitational constant (m s^{-2}) and p is pressure (hPa). The integral bounds represent the surface (s) and boundary pressures (b). The scaling term ζ is adjusted to fit the TPW data to the integrated moisture at the analysis gridpoint closest to the radiometer site. Once the scaling term has been derived, it is applied above the boundary layer throughout the remainder of the domain. We assume that the surface moisture that is mixed into the boundary layer is representative of the low-level moisture since it is analyzed from surface dewpoint data in real time.

4.3 Horizontal Shape Matching

To distribute the structure from the three LPW fields into the 21 LAPS pressure levels a technique known as horizontal shape matching (HSM) is used, Birkenheuer 1994. The operational HSM equation valid at a particular LAPS level is

$$\begin{aligned} &\alpha\nabla^4\phi \;-\; \beta\psi_x\phi_x \;-\; \beta\psi_y\phi_y \;-\; \beta\psi\nabla^2\phi \;+\; \gamma\phi \\ &\qquad = \;-\sum_{i=1}^{3}\beta_i\left[\psi_x\phi^g_{ix} \;+\psi_y\phi^g_{iy} \;+\psi\nabla^2\phi^g_i\right] \;+\; \gamma\phi' \;, \end{aligned} \qquad (3)$$

where ϕ is the desired function, ϕ^g is the field containing gradient information, and ϕ' is a background field. The terms α, β, and γ weight the response of the Laplacian (smoothing), gradient structure, and background respectively. The x and y subscripts denote partial derivatives. Note that the β term can be a function of x and y, because in our satellite application the β term depends on clear fraction ψ, a function in both x and y, and in addition is subscripted with i that denotes a particular LPW level.

The β term in the HSM equation can be divided into three parts corresponding to each LPW level: β_1, β_2, and β_3. Their sum is constrained to equal β as follows. For a specific LAPS level, we describe $\beta = \sum \beta_i$ where $\beta_i = f_i \beta$ and

$$\sum f_i = 1. \tag{4}$$

β_i effectively distributes the structure from the three LPW layers (ϕ_i^g) at the level of interest. Table 1 lists the various fractional weights (f_i) applied to the precipitable water layer as it relates to each LAPS pressure level. Though this treatment permits all three precipitable water layers to influence any LAPS pressure level, at this time only the two adjacent precipitable water layers apply to each LAPS pressure level; the f_i values used produce a linear interpolation of structure in the vertical.

Table 1. GOES weighting parameters

LAPS Pressure level (hPa)	fraction f_i used		
	i=1	i=2	i=3
900	1.00	0.00	0.00
850	1.00	0.00	0.00
800	1.00	0.00	0.00
750	0.42	0.58	0.00
700	0.00	1.00	0.00
650	0.00	0.82	0.18
600	0.00	0.68	0.32
550	0.00	0.52	0.48
500	0.00	0.38	0.62
450	0.00	0.23	0.77
400	0.00	0.09	0.91
350	0.00	0.00	1.00
300	0.00	0.00	1.00

Equation 2 can be solved numerically using over relaxation techniques. If the ψ term is zero (total cloud situation), no gradient structure will be added to the analysis because nothing would be gained by this step. Therefore, one of the first steps in the analysis integrates ψ to evaluate the percentage of the scene that is clear. If less than 33% of the scene is clear the HSM step is skipped.

4.4 Cloud Saturation

Clouds indicate saturated air. The LAPS 3-D cloud analysis is used to infer moisture above the amounts analyzed to this point in the moisture algorithm. The current algorithm begins by computing the mean relative humidity, $\bar{RH}_k$ at each level (k) in the analysis. The relative humidity is computed from the analyzed specific humidity, ambient temperature, and pressure.

The analysis continues by performing the following at each i, j gridpoint at a specific level, k. Keep in mind that each pressure level is treated uniquely by the algorithm. If the cloud fraction, $cg_{i,j,k}$ is greater than 0.6, we assume clouds should be influencing the RH. A linear model of RH is obtained directly from the cloud amount from the relationship

$$RH^{guess}_{i,j,k} = cg_{i,j,k} + \bar{RH}_k(1 - cg_{i,j,k}) \tag{5}$$

where we see that given total cloud cover, we have saturated RH. Anything less than total cloud cover will offer an RH value that would ramp linearly down to the mean RH of the domain if it were not for the fact that this linear function is not applied for $cg_{i,j,k}$ values less than 0.6. The $RH^{guess}_{i,j,k}$ value is applied to the gridpoint only if it is greater than the original $RH_{i,j,k}$. The new set of specific humidity values is computed from the new cloud influenced relative humidity field.

4.5 Quality Control

The final step in the algorithm is quality control. Each moisture value is compared to the LAPS analyzed temperature, and if supersaturated, it is reported and reduced to saturation.

5. IMPACT STUDY

Two basic datasets were chosen. The first (radiometer) extended between 1 January 1994 and 14 November 1994. This dataset consisted of runs where radiometer data would have been used if available. There are no guarantees that radiometer data were used in every run in this time period since it was not possible to single out only radiometer versus no-radiometer runs in this dataset. However, it is reasonable to assume that more than 80 % of these runs were made with radiometer data available.

The second dataset spanned 15 November 1994 to 10 April 1995. Radiometer data were unavailable in this time frame. In both datasets, satellite modifications to the fields were not applied, however, all other adjustments were made using the nominal data sources available to the moisture fields. Along the way there were some changes to LAPS in general but no major modifications were made to the moisture analysis. RUC data, initially from FSL and later from the National Centers for Environmental Prediction (previously NMC) were used as the background field.

5.1 Computed Statistics

The data were studied in two different ways. First they were plotted and example plots appear in this report for 800, 700, 500, and 100 hPa. For each pressure, a scatterplot shows a LAPS and radiosonde observation (RAOB) dewpoint comparison (Figures 1-4).

For each pressure level and dataset (with radiometer and without radiometer) a difference statistic was computed (LAPS-RAOB). It should be noted that the RAOB data used were from the Weather Service Forecast Office (WSFO) in Denver, CO, and that the RAOB data were not included in the analyses being assessed. The difference statistic is a measure of bias, positive indicates that LAPS is more moist than RAOB. The standard deviation of the difference statistic is indicative of the scatter seen in the plots. Furthermore, the difference statistics can be used to determine whether the bias differences seen between the radiometer and no-radiometer datasets are real by applying a Student-T test. Shown in Table 2 are the bias and standard deviation for each dataset and the Student T statistic including the degree of freedom and the probability that the two distributions are the same, stratified by pressure level.

Table 2. Statistical Results

Pressure Level (hPa)	Radiometer bias (K)	Radiometer σ (K)	no-Radiometer bias (K)	no-Radiometer σ (K)	D.F.	Student T T-statistic	Prob.
800	1.717	3.007	2.688	3.115	593	3.850	1.31e-04
700	1.017	3.264	2.226	3.255	655	4.663	3.78e-06
500	1.684	4.572	3.085	4.519	652	3.862	1.24e-04
100	1.654	4.707	4.723	3.415	533	8.573	1.09e-16

5.2 Discussion

Figures 1 through 4 illustrate the change in scatter as we go through the atmosphere. We see scatter increasing as we go farther from the surface. Plotted on each scatter diagram is also the linear least-squares fit line, and we see that generally it is offset from the best fit (45 degree) line also plotted. In all but the 100 hPa case, the best fit line shows lower bias at the colder end of the plot. Contrasting the individual best fit lines between the radiometer and no-radiometer datasets does not appear to show any great differences except at 100 hPa where there is so much scatter present that a least-squares fit loses its meaning (Figure 4). For this level it may instead be better to rely on the difference statistic (bias) to show such trends. Between 800-500 hPa the best fit lines in the radiometer sample appear to be improved over the no-radiometer dataset.

The bias statistic and its analysis with the Student-T test shows a clear positive impact of the radiometer data (Table 2). Both populations have approximately the same variance, but the radiometer dataset has a lower bias on the order of a degree K, a desirable outcome.

6. SUMMARY

The LAPS moisture analysis using radiometer data had a lower bias in dewpoint temperature with respect to the Denver RAOB. This was true for all levels shown, however, it could be argued that the 100 hPa level was not improved based on the greater scatter in the data. Therefore, the current technique of using the radiometer to scale the analysis seems to work for the middle and lower troposphere. During the last two years there have been many improvements to LAPS that could possibly affect this study. However, if these improvements had significant impact on the moisture analysis, then no-radiometer dataset would have shown a lower bias. But, since in this later time period it showed poorer agreement to RAOB data two probable reasons for this result would be that the radiometer data led to an improvement, or the weather differences in the datasets were responsible for the results. Only an expanded study or a more controlled study where the same days are analyzed with and without radiometer data will reduce the likelihood of the second factor. The latter of these would be preferred if it were possible.

Scatter in the data, represented by σ in the difference statistic, in effect is the same for both datasets. This would be the expected impact of the radiometer adjustment, since it scales the data to reduce bias but is not addressing the overall uncertainty in the analysis.

In the future, GPS data will augment or replace radiometer data. Currently GPS data are not offered in real time, however, plans are to begin testing LAPS with this data source. Initially these data would be applied the same way we now use radiometer data. With more datasets, however, we plan to broaden the application of total column water vapor data. In the meantime, this study represents a very rudimentary and simplistic application of these data types.

7. REFERENCES

Birkenheuer D., 1994: The positive impact of GOES-7 data in the LAPS water vapor analysis. *Preprints, Seventh Conference on Satellite Meteorology and Oceanography*, Monterey, CA, American Meteorology Society, Boston, 400-403.

Birkenheuer, D., 1991: An algorithm for operational water vapor analyses integrating GOES and dual-channel microwave radiometer data on the local scale. *J. Appl. Meteor.* **30**, 834-843.

Han, Y., J.B. Snider, E.R. Westwater, S.H. Melfi and R.A. Ferrare, 1994: Observations of water vapor by ground-based microwave radiometers and Raman lidar. *J. Geophys. Res.*, **99**, 695-702.

McGinley, J.A. and S.C. Albers, 1991: Validation of liquid cloud water forecasts from the Smith-Feddes method derived from soundings and LAPS analyses. *Fourth AMS International Conference on Aviation Weather Systems*, 24-26 June 1991, Paris, France, 228-233.

McGinley, J.A., S. Albers and P. Stamus, 1991: Validation of a composite convective index as defined by a real time local analysis system. *Wea. Forecasting*, **6**, 337-356.

Rogers, R.R. and A.P. Schwartz, 1991: Mesoscale Fluctuations of Columnar Water Vapor, *J. Appl. Meteor.*, **30**, 1305-1322.

Westwater, E.R., 1993: Ground-based remote sensing of meteorological variables, in *Atmospheric Remote Sensing by Microwave Radiometry*, edited by M.A. Janssen, John Wiley, New York, 145-213.

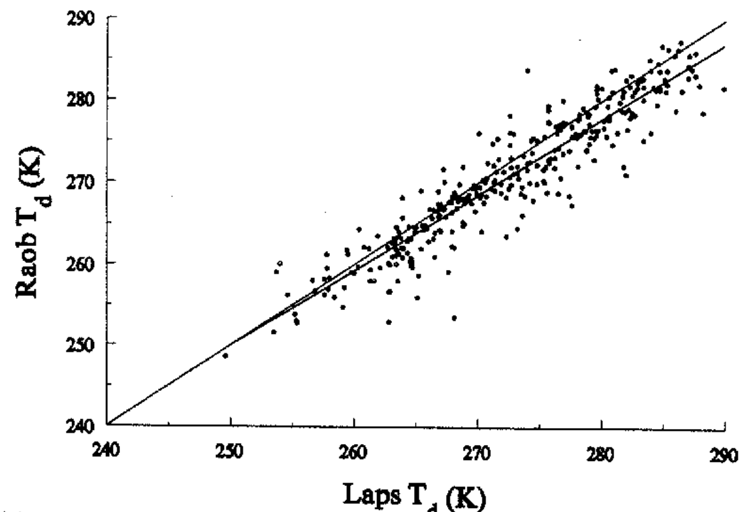

(a) 800 hPa with radiometer

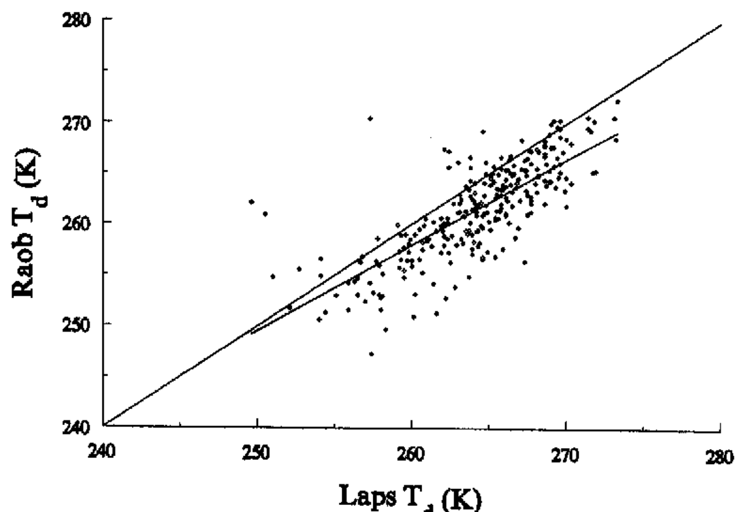

(b) 800 hPa without radiometer

Fig 1. The 800-hPa LAPS and RAOB dewpoint data. (a) where radiometer data were incorporated into the analysis. (b) where radiometer data were excluded from the analysis. Also plotted are the linear least-squares fit to the data in both.

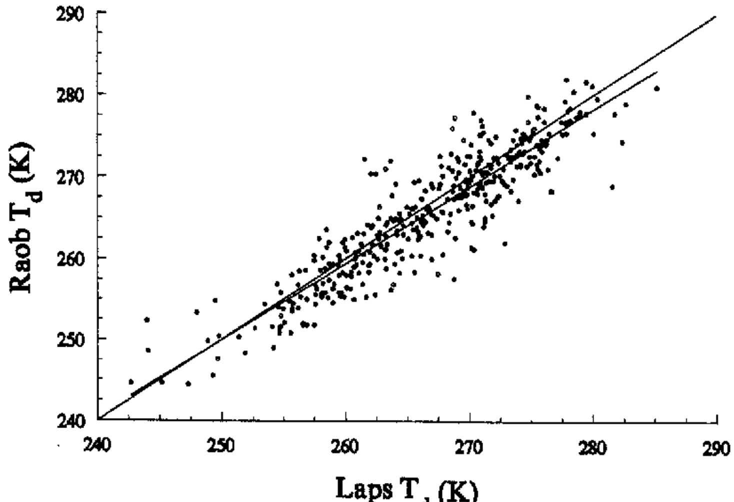

(a) 700 hPa with radiometer

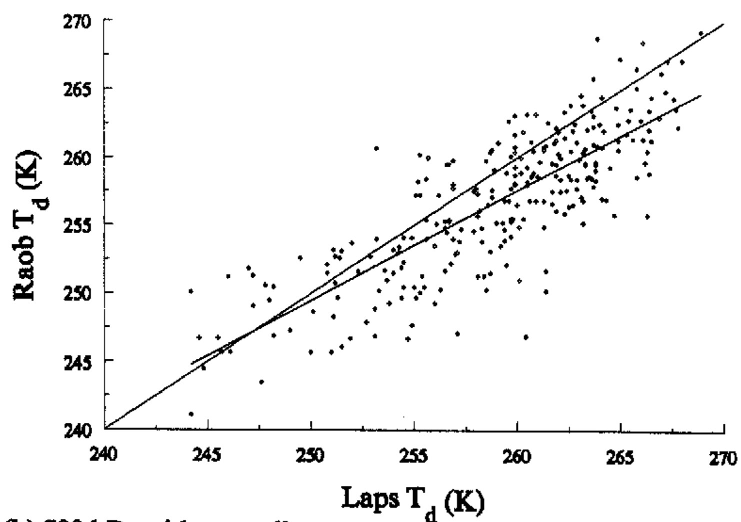

(b) 700 hPa without radiometer

Fig 2. The 700-hPa LAPS and RAOB dewpoint data. (a) where radiometer data were incorporated into the analysis. (b) where radiometer data were excluded from the analysis. Also plotted are the linear least-squares fit to the data in both.

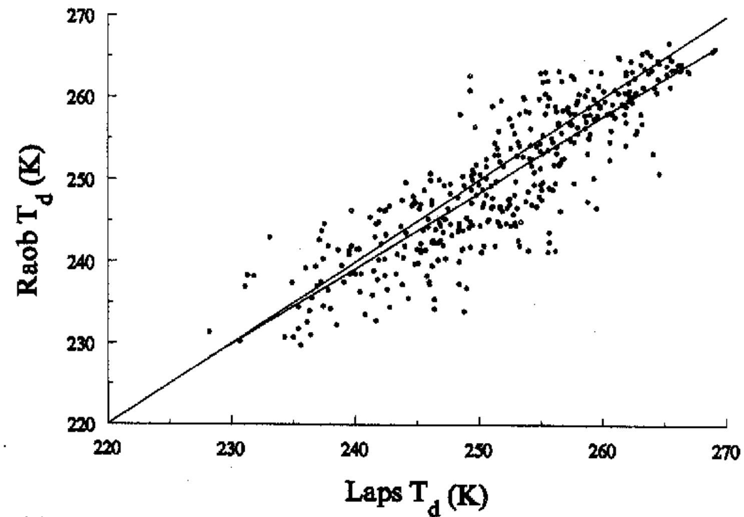

(a) 500 hPa with radiometer

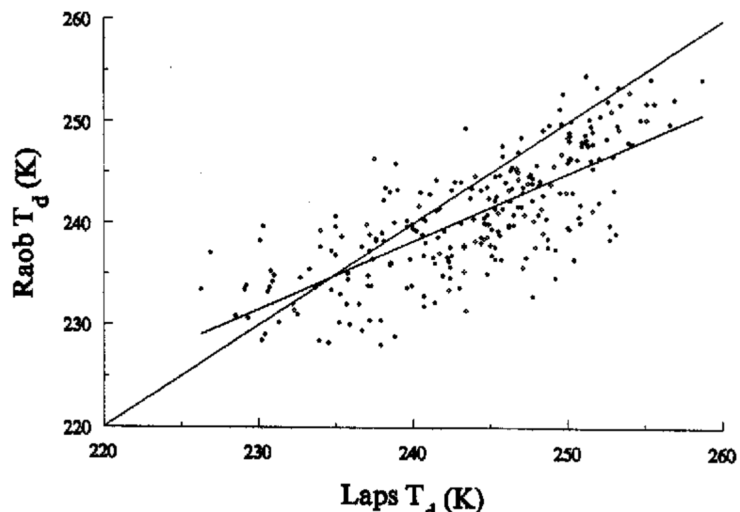

(b) 500 hPa without radiometer

Fig 3. The 500-hPa LAPS and RAOB dewpoint data. (a) where radiometer data were incorporated into the analysis. (b) where radiometer data were excluded from the analysis. Also plotted are the linear least-squares fit to the data in both.

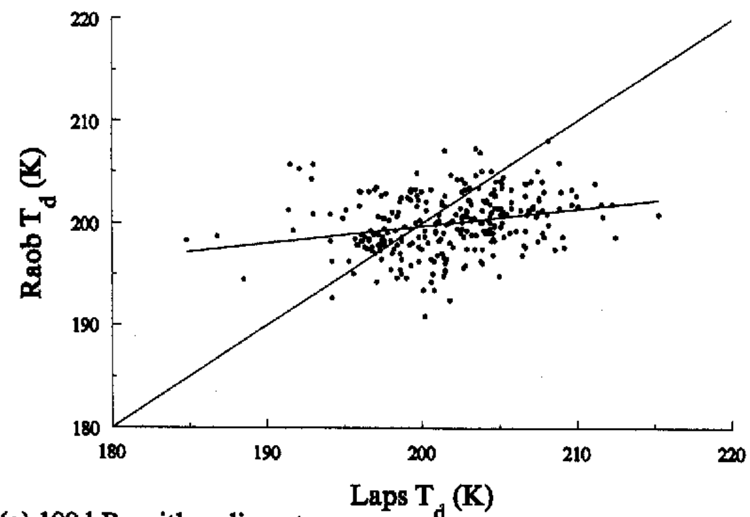

(a) 100 hPa with radiometer

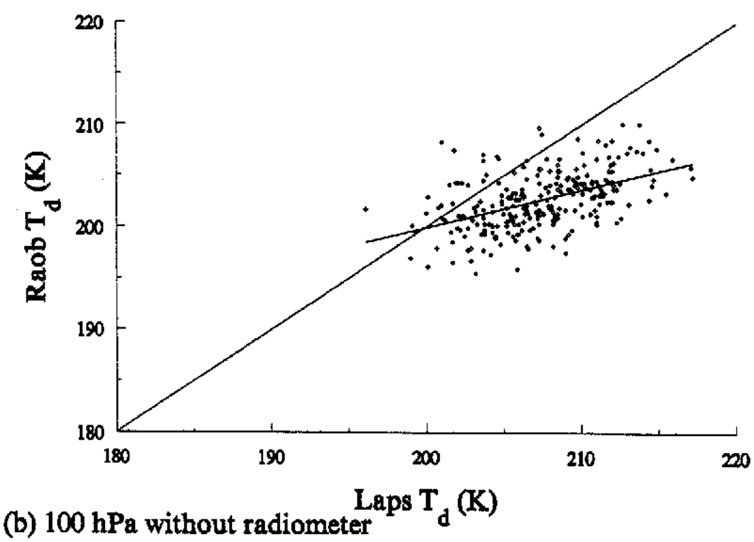

(b) 100 hPa without radiometer

Fig 4. The 100-hPa LAPS and RAOB dewpoint data. (a) where radiometer data were incorporated into the analysis. (b) where radiometer data were excluded from the analysis. Also plotted are the linear least-squares fit to the data in both.

*U.S. GOVERNMENT PRINTING OFFICE 1998-0-673-018/40081